[5]The result obtained using our definition of diffraction is in good agreement with the value 1.20 ± 0.19 mb of Barish *et al.*, Ref. 2, obtained from an analysis of the MM^2 peak.
[6]M. Derrick *et al.*, Phys. Rev. D 9, 1215 (1974).
[7]S. Barish *et al.*, Phys. Rev. D 9, 1171 (1974).
[8]The difference in resolution of the MM^2 and the $p\pi^+\pi^-$ effective mass does not affect this conclusion.
[9]F. T. Dao *et al.*, Phys. Rev. Lett. 30, 34 (1973) have studied inclusive Δ^{++} production in 303-GeV/c pp interactions.

PHYSICAL REVIEW D VOLUME 9, NUMBER 7 1 APRIL 1974

Search for fractionally charged particles photoproduced from copper*

R. Galik,† C. Jordan,‡ B. Richter, E. Seppi, and R. H. Siemann†
Stanford Linear Accelerator Center, Stanford University, Stanford, California 94305

S. D. Ecklund
National Accelerator Laboratory, Batavia, Illinois 60510
(Received 7 December 1973)

A search for fractionally charged particles photoproduced from copper has been performed. No such events were detected. Lower limits for the mass of the quark established by this experiment are as follows: $m_{\text{charge}=1/3} > 3.6$ GeV/c^2 and $m_{2/3} > 4.5$ GeV/c^2, if the quark interacts strongly and if the Drell model of hadron photoproduction applies to quarks; $m_{1/3} > 1.4$ GeV/c^2 and $m_{2/3} > 1.8$ GeV/c^2, if the quark does not interact strongly ("leptonic" quark).

I. INTRODUCTION

Since the development of symmetry ideas based on a triplet of fractionally charged particles, quarks,[1] there have been many attempts to discover a real particle of fractional charge. The experimental techniques of these searches are varied, including chemical[2] and cryogenic[3] techniques as well as particle-counting techniques. The latter have been used for both cosmic-ray and accelerator experiments. Although some positive results have been reported,[4] they have not withstood criticism.[5] At the present time, the most stringent upper limits on quark-production cross sections and lower limits on quark masses come from the accelerator experiments.[6]

Interpretation of a null result in any of these experiments is extremely uncertain because the dynamics of quark production are not known. At least one particular model, the statistical model of Hagedorn,[7] makes very pessimistic predictions for the cross section for the production of high-mass quarks in hadron-hadron collisions. In this model, the cross section for production of quark-antiquark pairs depends on the mass m as

$$m^n e^{-2m/T},$$

where $T \simeq 160$ MeV/c^2 and is independent of incident energy, and n, which is in the range of 3 to 5, depends on details of the quark spectrum. For high masses, the cross section drops an order of magnitude as the mass increases by 190 MeV/c^2.

Consider for example the result of Antipov *et al.*[8] for a beam energy of 70 GeV, a secondary momentum (for singly charged particles) of 50 GeV/c, and an angle of 0 mrad. The experimental result is the observation of no quarks while approximately 10^9 π^- mesons were detected. Using the measured π^- cross section, an upper limit for the differential cross section for production of charge-$\frac{2}{3}$ quarks at 33.3 GeV/c is determined to be

$$\frac{d^2\sigma}{d\Omega\, dp} < 7.7\times10^{-6}\ \frac{\mu b}{\text{sr GeV}/c}\ .$$

To interpret this result Antipov *et al.*[8] consider only the phase space for the reaction $N+N \to N+N+Q+\bar{Q}$ and conclude that the total cross section for production of quarks with mass 4.5–5 GeV/c^2 does not exceed 4×10^{-7} μb. An alternative interpretation of this result is to relate to the limit for the differential cross section to the π^- cross section by using the data of Bushnin *et al.*[9] and the statistical model. The result is that the quark would not have been detected if its mass is greater than 2.5 GeV/c^2. Hence even though quark-antiquark production may be above threshold, the cross section may be so small that no events were detected. Because the temperature in the model T does not depend on incident energy, the same conclusion would be true for experiments at the CERN ISR and at NAL.

While the statistical model may not correctly

describe quark-antiquark production in hadron-hadron collisions, it should be recalled that it gives an approximate description of particle-production ratios.[7] The predictions of this model are sufficiently discouraging that we felt the possibility of quark production in photon-initiated reactions should be investigated. The Drell model[10] provides an approximate picture of particle production in photon reactions.[11] The cross section for production of a spin-0 particle in this model is

$$\frac{d^2\sigma}{d\Omega\, dp/p} = \frac{\alpha}{2\pi} Q^2 \frac{E^2(k-E)}{4\pi k^3} \times \frac{4\theta^2}{[(m/E)^2+\theta^2]^2} \sigma_{\text{tot}}(k-E)\,, \qquad (1)$$

where θ is the production angle, $\sigma_{\text{tot}}(k-E)$ is the total quark-nucleon cross section, Q is the particle charge, and other quantities are defined in the Feynman diagram for the process (Fig. 1). The mass dependence of this model is much less extreme than that of the statistical model. Two specific comments should be made about the above equation: First, the matrix element used to derive the cross section is not gauge-invariant. A gauge-invariant extension of this model by Stichel and Scholz[12] for the reaction $\gamma p \to \pi\Delta$ predicts a larger cross section than the Drell model. Second, an additional factor of order unity, which is dependent on the anomalous magnetic moment of the produced particle, multiplies this cross section when considering production of spin-$\frac{1}{2}$ particles.[10]

To attain large center-of-mass energies with a photon beam at SLAC (Stanford Linear Accelerator Center), it is necessary to use a complex nucleus as a target. The use of the internal motion of the nucleons in the nucleus to increase the center-of-mass energy is not a new idea, as it has been used in previous particle searches.[13] Danos and Gibson[14] have published theoretical estimates for the probability of having a high-momentum component in the nucleus. These estimates together with a cross section calculated in the Drell model indicate that quarks in the 2–4 GeV/c^2 mass range would be produced in sufficient quantities to be detected at SLAC.

Quark searches have been performed at several electron accelerators including SLAC,[15] but these experiments have been designed primarily to detect "leptonic" quarks.[16] In each of these experiments many collision lengths of material were placed between the production target and the detectors. Since the production mechanisms in photon-initiated reactions may be complementary to that in proton-proton collisions, and since no search for strongly interacting quarks has been performed at an electron accelerator, we have done so.

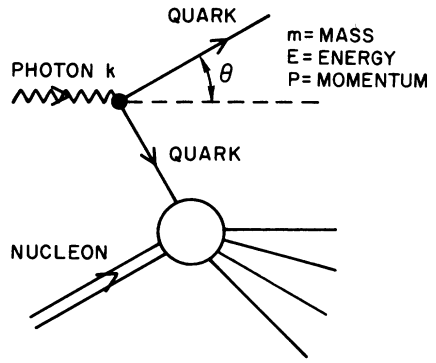

FIG. 1. Diagram for Drell-model production of quarks.

The theoretical uncertainties in interpreting the results of this experiment are as great as in the hadron-initiated experiments, but at least are different. Hadron- and photon-initiated reactions taken together can give more confidence to a conclusion than either can separately.

II. EXPERIMENTAL DESCRIPTION

This experiment was performed in End Station A at SLAC. A schematic of the beam line is shown in Fig. 2. A high-energy, high-intensity electron beam was incident on a bremsstrahlung radiator of either 0.0285 or 0.1069 radiation lengths. The electron-beam current was measured to an accuracy of ±1% by a precision toroid[17] before striking the radiator; this current measurement served as the primary monitor of the beam flux. After the radiator the electrons were bent out of the beam line. The photon beam was collimated twice before reaching the target; each collimator was followed by a magnet to remove charged particles from the beam. The beam also passed through an ion chamber and a thin Čerenkov monitor[18]: the latter gave a reliable secondary measurement of the beam flux. The photon beam was incident on one of two copper targets (0.638 ± 0.005)- and (1.257 ± 0.008)-cm thick, and then dumped in a water-cooled tungsten block downstream of the target.

The relation between the primary electron-beam current and the photon flux has been measured during several previous experiments for a standard radiator (0.0285 radiation length) and standard beam-collimator settings. Under these conditions it is known that 0.0215 ± 0.0010 of the electron-beam power is in the photon beam.[19] The energy spectrum of the photon beam can easily be calculated.[20] When a nonstandard radiator or nonstandard collimator settings were used, the Čerenkov

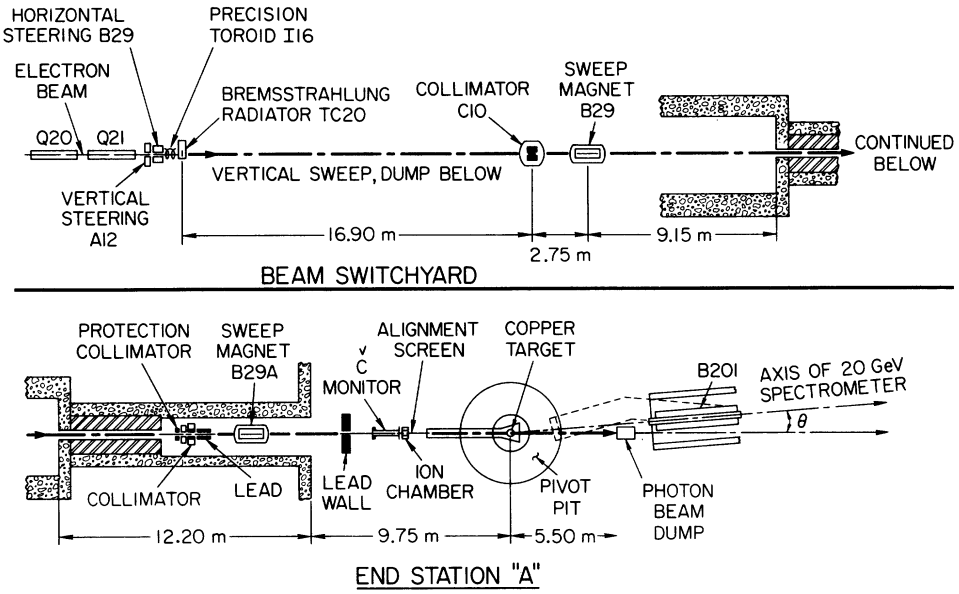

FIG. 2. The photon-beam line.

monitor, which was calibrated under the standard conditions, was used to determine the new ratio of beam powers.

Particles produced in the target were detected with the SLAC 20-GeV spectrometer.[21] The length of the particle flight path from the target to the momentum focus of the spectrometer (see Fig. 3) is approximately 43 meters. The spectrometer detector was equipped with a specially constructed set of trigger and hodoscope counters. The configuration of these counters is shown in Fig. 3. Five thick scintillators (made of NE102 and equipped with Amperex 56 DVP phototubes) were used to make ionization measurements for each particle. The light pipes of these counters were oriented such that it was not possible for a particle to pass through more than two light pipes. Five planes of 1.27-cm-thick hodoscopes (overlapped to give 2-cm-wide bins) were used to measure particle position. These hodoscopes were used to be sure that particles did not pass through the light pipes or near the edges of the thick counters and to reconstruct the particle trajectory through the detector. Three hodoscopes were necessary to obtain a redundant measurement of the vertical trajectory because of the large angular dispersion in the vertical. In the horizontal, all trajectories coming through the spectrometer are approxi-

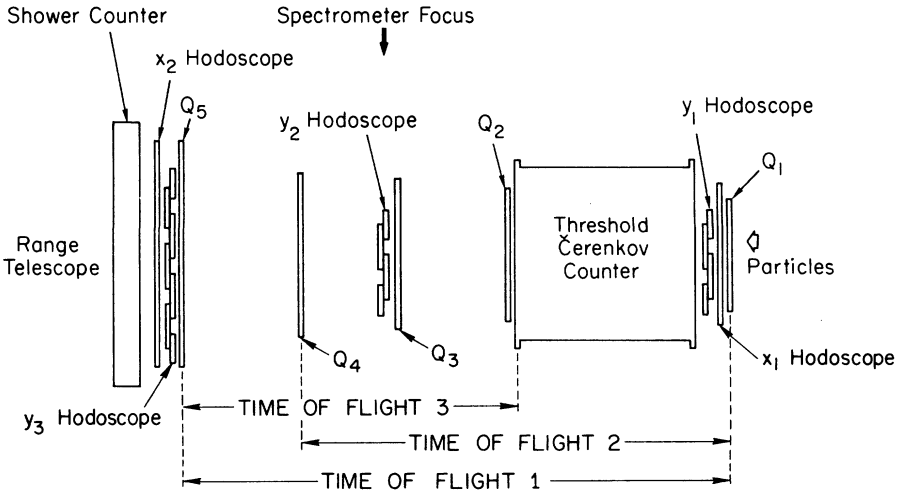

FIG. 3. Schematic diagram of the detector.

mately parallel, and therefore only two hodoscopes are needed for a redundant measurement.

In addition to the thick scintillators and hodoscopes, the spectrometer was equipped with a threshold Čerenkov counter (with sufficient gas pressure to count protons at the spectrometer momentum), a lead-scintillator shower counter, and a range telescope.

The thick scintillators and hodoscopes were built with high-linearity phototube bases to ensure that the tube response was linear for pulses of currents up to 300 mA (−15 volts into 50 ohms). Typical relativistic particles produced pulses 3–4 volts in amplitude; hence the phototube response was linear over the expected range of pulse heights. The response of a typical counter was checked with cosmic rays by making a pulse-height analysis of the counter response for different counter high voltages. It was verified that the counter had the expected gain characteristic for pulses up to 6.5 volts in amplitude.

The mean value of energy loss ($\bar{\Delta}$) of a charge-$\frac{1}{3}$ particle of 6.67-GeV/c momentum in a 5.08-cm-thick scintillator is plotted as a function of particle mass in Fig. 4. This calculation includes the density-effect correction and uses the parameters of Sternheimer[22] for $(CH)_2$. The minimum mean energy loss occurs at a mass of 2 GeV/c^2. For this value of mass, the distribution of energy loss[23] is plotted in Fig. 5. Figure 5 also shows the energy-loss distribution for a relativistic muon.

From these energy-loss distributions, it is seen that for a counter to be efficient for all possible quark masses, it must be efficient for muons when the counter signals are attenuated by a factor of 12. All discriminator levels for the thick scintillators were set so that the most probable energy loss for muons was a factor of 30 above the threshold. This insures greater than 0.99 efficiency for charge-$\frac{1}{3}$ particles. All hodoscope high voltages were set to a voltage 200 volts above the knee in a plateau curve taken with a factor of 12.6 attenuation in the signal.

Both anode and dynode signals from each thick scintillator were used. After inverting, the dynode signal was used for both a discriminator input and the input to a camera system to be described below. The anode signal was used as the input to two analog-to-digital converters (ADC's).[24] By use of a resistive signal splitter, the effective gains of these ADC's were in the ratio of 9:1. Thus one ADC was sensitive to the pulse height expected for charge $\frac{1}{3}$, the other to that expected for charge 1.

The event trigger was a fivefold coincidence between the scintillation counters. The timing was such that events with velocities down to 0.55c would make a coincidence, and it was symmetric about a velocity of c to allow subtraction of accidental events. A subsequent circuit limited the trigger rate to one per SLAC pulse. To avoid accidental coincidences in the hodoscopes and ADC's caused by the loose trigger timing, the trigger signal was put into coincidence with signals from Q_1, Q_3, and Q_5, where these latter signals

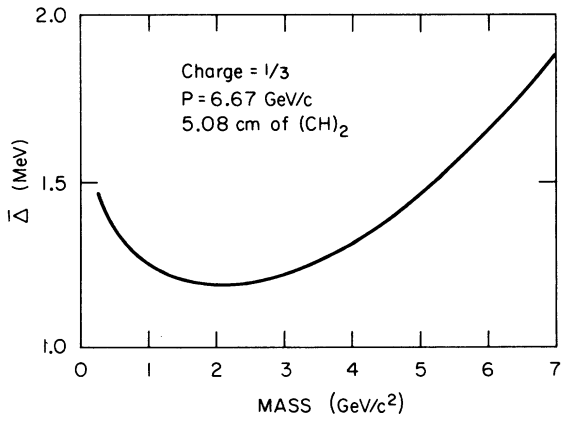

FIG. 4. The mean value of energy loss ($\bar{\Delta}$) for a charge-$\frac{1}{3}$ particle passing through 5.08 cm of scintillator.

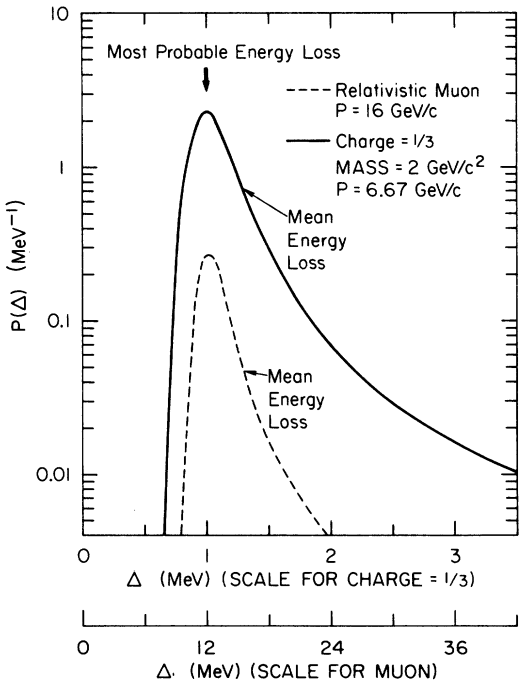

FIG. 5. The distributions of energy loss in a 5.08-cm-thick scintillator for a quark with the minimum mean energy loss and for a relativistic muon. The probability for an energy loss between Δ and $\Delta + d\Delta$ is $P(\Delta)d\Delta$. These distributions include the effects of light-collection variation and photon statistics on measurement of Δ.

determined the timing. The resultant coincident signals were used to gate the hodoscopes and ADC's.

A resistive signal splitter divided each hodoscope signal into two with a ratio of amplitudes of 0.88 : 0.12. Each of the resultant signals was input to a discriminator; thus each hodoscope element was pulse-height analyzed with a three-channel pulse-height analyzer.

The time of flight between pairs of counters was digitized (using EG&G TH200A/N time-to-amplitude converters). This allowed several checks on an event: First, the three times of flight must be consistent, and second, the particle velocity determined by time of flight must agree with that determined from the ionization measurements in the thick scintillators. The calibrations of the time-of-flight units and pulse-height-analysis systems were checked four to six times each day. No significant changes in calibration or resolution were observed.

Additional information on the pulse heights of the shower and Čerenkov counters and the contents of the range telescope were read in with each event. The event reading, recording, on-line analysis, and off-line analysis were performed with an XDS 9300 computer.

When the trigger rate was low, a photograph was taken of the pulses from the five scintillators. The dynode pulses were delayed relative to each other (approximately 250 nsec between pulses), added together, and displayed on a scope. The resultant trace was photographed. This photograph allowed one to form a qualitative impression of an event. Quantitative measurements were left to the digitizers described previously.

The signature of a quark in this apparatus would be:

(1) a good trajectory in both the horizontal and vertical (this trajectory would be detected only by the low-threshold hodoscope discriminators, would be within the spectrometer acceptance, and would not pass near the edges or light pipes of any of the thick scintillators);

(2) pulse heights in each of the five scintillators which are consistent with those expected from a particle of definite charge, mass, and momentum (this consistency can be measured by using the probability distributions for ionization loss[23]);

(3) times of flight consistent with each other and the mass determined from the ionization measurements; and

(4) a signal on the Čerenkov counter consistent with the measured velocity (no clear interpretation could be made of the shower-counter and range-telescope signals).

The functioning of the apparatus was checked by simulating quarks with attenuators in the trigger counter and hodoscope signals. The result of this check was that 53% of all triggers were correctly identified by the apparatus and analysis programs. This identification included passing all the tests described above. Of the triggers that failed, 6% were discarded events, 23% were outside the spectrometer acceptance or near a light pipe or counter edge, and 6% did not have good tracks through the detector. Thus our efficiency for detecting a quark satisfying the above criteria was approximately 82%. Most of the inefficiency (15%) was due to zero or two hits in one of the five hodoscopes.

The acceptance of the spectrometer was determined by a combination of calculation and measurement. The acceptance of a small region of the aperture was calculated by Monte Carlo technique. This region was defined by the hodoscopes and was chosen such that all trajectories passing through it would not pass near magnet pole pieces or defining slits. A data run was then used to determine the ratio of the number of counts in the full aperture (passing all data cuts) to those within the restricted region. The spectrometer acceptance was thus determined to be

$$\Delta\Omega \frac{\Delta p}{p} = (5.77 \pm 0.27) \times 10^{-6} \text{ sr};$$

the error includes the statistical error of the Monte Carlo calculation. For part of this experiment the spectrometer was operated at higher magnet excitation than ever previously, in fact, at excitations beyond the range of magnetic measurements. A measurement of pion photoproduction at low missing mass and at several incident energies verified that the acceptance did not have any detectable momentum dependence over the range of this experiment.

III. RESULTS

Data were taken at several different angles and momenta as shown in Table I. No events were detected with the signature of a quark as described above. In the final analysis all events which passed only the requirement of a pulse height less than that corresponding to a certain value of energy loss in three of the five counters were examined. This energy-loss value was 10 MeV in the 5.08-cm-thick counters and 7.5 MeV in the 3.81-cm-thick counters. None of these events could be identified as a quark because in all cases at least two of the criteria of a quark were violated. The 90%-confidence-level upper limits for the cross sections are given in Table I.

We have used two models to obtain estimates

TABLE I. 90% confidence limit on the quark-production cross section.

Data-point number	θ[a]	p[b]	E_0[c]	X[d]	T[e]	E.Q.[f]	$\frac{d^2\sigma}{d\Omega(dp/p)\,\text{E.Q.}}\Big\|_{90\%}$[g]
1	1.26	−21.0	19.99	0.0285	0.638	1.57×10^{17}	4.7×10^{-5}
2	7.00	−17.5	20.72	0.1069	1.257	8.80×10^{16}	4.2×10^{-5}
3	7.00	−17.5	20.47	0.0285	1.257	3.08×10^{16}	1.0×10^{-4}
4	7.00	17.5	20.72	0.1069	1.257	2.22×10^{16}	1.7×10^{-4}
5	7.00	18.5	20.72	0.1069	1.257	3.82×10^{16}	9.7×10^{-5}
6	7.00	12.0	20.72	0.1069	1.257	7.20×10^{16}	5.2×10^{-5}

[a]The spectrometer angle in degrees.
[b]The spectrometer momentum in GeV/c for a unit-charge particle. The sign indicates the charge of the detected particles.
[c]The photon-beam endpoint energy in GeV.
[d]The photon-radiator thickness in radiation lengths.
[e]The copper-target thickness in cm.
[f]The number of equivalent quanta incident on the target. This figure is corrected for pair production in the target.
[g]The 90%-confidence-level upper limit to the quark-production cross section on a copper nucleus. The units are μb sr^{-1} (equivalent quantum)$^{-1}$.

of the lower limit for the mass of the quark which can be accommodated by these data. The first is the Drell model[10] with the distribution of Danos and Gibson[14] used to estimate the probability for high-momentum components in the nucleus. A total quark-nucleon cross section of 10 mb has been assumed. The calculation is discussed in detail in the Appendix, and the 90%-confidence-level lower limits for the quark mass are presented in Table II.

These lower limits are based on a mean of 2.3 events at each of the data points. Within the model, the 90%-confidence-level lower limits can be determined for the entire experiment. The results are $m_{1/3} > 3.6$ GeV/c^2 and $m_{2/3} > 4.5$ GeV/c^2.

To determine the lower limits for the mass of the "leptonic" quark, we have used the Weizsäcker-Williams approximation to the Born amplitudes as discussed by Kim and Tsai.[25] Both the elastic and quasielastic contributions have been calculated using the form factors as parameterized by Kim and Tsai. The cross section for this process depends on the fourth power of the quark charge and is approximately exponential in the quark mass as is shown in Fig. 6. Within this

TABLE II. 90%-confidence-level lower limits for the quark mass using the Drell model (Ref. 10) and the probability distribution of Danos and Gibson (Ref. 14). $E_0 \equiv$ endpoint energy of spectrum in GeV. $P_{1/3(2/3)} \equiv$ momentum of charge-$\frac{1}{3}$ ($\frac{2}{3}$) quark, in GeV/c. $m_{1/3(2/3)} \equiv$ 90%-confidence-level lower limit for the mass of the charge-$\frac{1}{3}$ ($\frac{2}{3}$) quark in GeV/c^2.

Data-point number	E_0	$P_{1/3}$	$m_{1/3}$	$P_{2/3}$	$m_{2/3}$
1	19.99	−7.00	2.6	−14.00	3.1
2	20.72	−5.83	3.3	−11.67	4.2
3	20.47	−5.83	3.0	−11.67	3.9
4	20.72	5.83	2.9	11.67	3.7
5	20.72	6.17	3.1	12.33	3.9
6	20.72	4.00	2.7	8.00	4.1
All data	•••	•••	3.6	•••	4.5

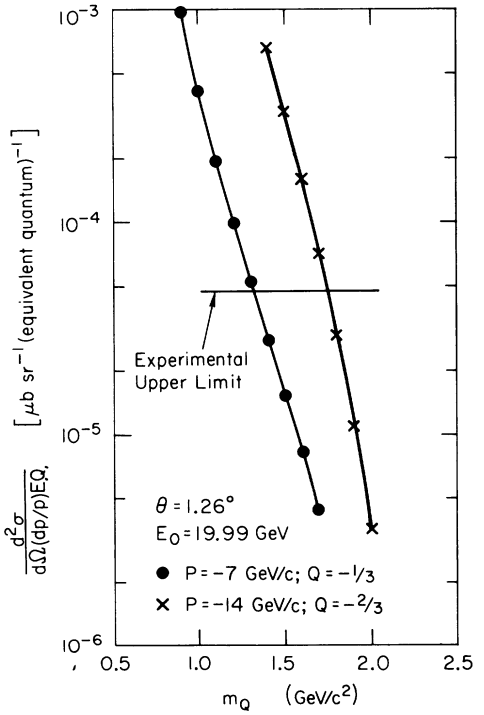

FIG. 6. The cross section per equivalent quantum as a function of quark mass for the first data point in the Kim and Tsai model. Both elastic and quasielastic contributions are included.

model, the 90%-confidence-level lower limits to the mass of the "leptonic" quark are: $m_{1/3} > 1.4$ GeV/c^2 and $m_{2/3} > 1.8$ GeV/c^2 (Table III).

IV. CONCLUSIONS

We have unsuccessfully searched for quarks photoproduced from copper. Model-dependent lower limits have been placed on the mass of the quark.

Although this search has been unsuccessful, photoproduction searches should be pursued at higher energies because the mass dependence of the photoproduction cross section may be much less severe than that of proton-proton collisions.

ACKNOWLEDGMENTS

We greatly appreciate the help of G. Fischer during the data collection for this experiment. We wish to thank D. Coward, D. Sherden, and C. Sinclair for their invaluable support. A. Golde and E. Taylor coordinated the preparation of the spectrometer and end station. L. Boyer, M. Browne, S. Coombes, S. Dyer, and A. Fillipi provided the necessary technical support. Finally, we wish to thank the SLAC accelerator crews for providing the necessary high-energy, high-intensity beams.

APPENDIX

The cross section per equivalent quantum for quark production in the Drell model is

$$\frac{d^2\sigma}{d\Omega(dp/p)\ \text{E.Q.}} = \int_{k_{\min}}^{E_0} n(k)\,\frac{d^2\sigma}{d\Omega\,dp/p}\,P\,dk\ .$$

In this equation E_0 is the endpoint of the spectrum, and $n(k)\,dk$ is the number of photons with energy between k and $k+dk$. $n(k)$ is normalized per equivalent quantum

$$\int_0^{E_0} kn(k)\,dk = E_0\ .$$

The Drell cross section, $d^2\sigma/d\Omega(dp/p)$, is given by Eq. (1) and is the cross section per nucleon. P, the probability per nucleus of finding a nucleon of sufficiently high momentum to make the reaction kinematically allowed, is determined from the model of Danos and Gibson.[14] The distribution published by Danos and Gibson, $P'(k_z)\,dk_z$, is the probability of finding a nucleon with a z component of momentum between k_z and k_z+dk_z. P' is normalized such that

$$\int_{-\infty}^{\infty} P'(k_z)\,dk_z = A\ ,$$

where A is the atomic weight of the nucleus. For large k_z, we have parameterized $P'(k_z)$ as

$$\log_{10}P'(k_z) = -1.14 - 4.16\log_{10}k_z - 1.10\,(\log_{10}k_z)^2\ ,$$

where k_z is in GeV and P' in GeV^{-1}. The distribution is spherically symmetric so one can determine the probability for having a total momentum of magnitude k_r to be

$$\rho(k_r) = \frac{-1}{2\pi k_r}\,\frac{dP'(k_r)}{dk_r}\ .$$

The probability P is given by

$$P = \int_\phi d\phi \int_{k_r} k_r^2\rho(k_r) \int_\theta \sin\theta\ \delta(\theta_N(k_r) - \theta)\,d\theta\,dk_r\ ,$$

TABLE III. 90%-confidence-level lower limits for the quark mass using the Weizsäcker-Williams method of Kim and Tsai (Ref. 25). $E_0 \equiv$ end-point energy of spectrum in GeV. $P_{1/3(2/3)} \equiv$ momentum of charge-$\frac{1}{3}$ ($\frac{2}{3}$) quark in GeV/c. $m_{1/3(2/3)} \equiv$ 90%-confidence-level lower limit for the mass of charge-$\frac{1}{3}$ ($\frac{2}{3}$) quark in GeV/c.

Data-point number	E_0	$P_{1/3}$	$m_{1/3}$	$P_{2/3}$	$m_{2/3}$
1	19.99	−7.0	1.3	−14.0	1.7
2	20.72	−5.83	1.1	−11.67	1.3
3	20.47	−5.83	0.9	−11.67	1.2
4	20.72	5.83	0.8	11.67	1.0
5	20.72	6.17	0.9	12.33	1.1
6	20.72	4.0	1.0	8.0	1.5
All data	•••	•••	1.4	•••	1.8

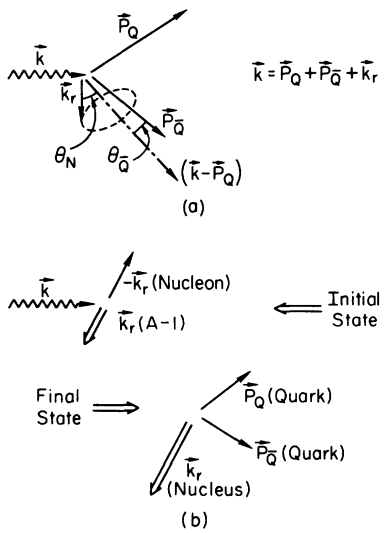

FIG. 7. (a) Definition of the momentum vectors in the kinematics. (b) Kinematics for Danos-Gibson quark photoproduction.

where θ_N is the angle between the missing-momentum vector $(\vec{k}-\vec{p}_Q)$ and the momentum of the recoiling nucleus $(\vec{k}_r)$, as shown in Fig. 7(a). The kinematics for the process $\gamma+A\rightarrow A+Q+\bar{Q}$ are used to calculate θ_N.

Evaluating the ϕ and θ integrals leaves

$$P=2\pi\int_{k_r(\min)}^{k_r(\max)}\sin\theta_N(k_r)\,k_r^2\rho(k_r)\,dk_r\ ,$$

where $k_r(\max)$ is large with respect to $k_r(\min)$, with momentum and energy conservation determining the former, and the latter being derived from the kinematics displayed in Fig. 7(b).

The four-momentum transfer to the nucleus is

$$t=2Am_p\{Am_p-[(Am_p)^2+k_r^2]^{1/2}\}\ .$$

The minimum four-momentum transfer ($|t|$) occurs when the undetected quark has momentum parallel to the missing momentum $(\vec{k}-\vec{p}_Q)$. Minimizing $|t|$ gives $k_r(\min)$, the minimum value for k_r.

The results of a typical calculation of the cross section are shown in Fig. 8.

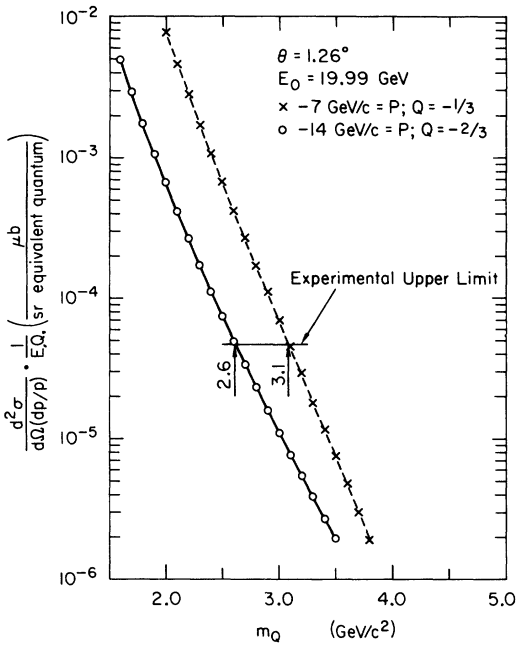

FIG. 8. The cross section per equivalent quantum versus quark mass in the Drell model.

*Work supported by the U. S. Atomic Energy Commission.

†Present address: Physics Department, Cornell University, Ithaca, New York 14850.

‡Present address: I. Physikalisches Institut, Aachen, West Germany.

[1]M. Gell-Mann, Phys. Rev. Lett. 8, 214 (1964).

[2]W. A. Chupka, J. P. Schiffer, and C. M. Stevens, Phys. Rev. Lett. 17, 60 (1966).

[3]A. F. Hebard and W. M. Fairbank, in *Proceedings of the Twelfth International Conference on Low Temperature Physics, Kyoto, 1970,* edited by Eizo Kanda (Academic Press of Japan, Kyoto, 1971).

[4]C. B. A. McCusker and I. D. Cairns, Phys. Rev. Lett. 23, 658 (1969); W. T. Chu, Y. S. Kim, W. J. Beam, and N. Kwak, *ibid.* 24, 917 (1970).

[5]D. S. Rahm and R. I. Louttit, Phys. Rev. Lett. 24, 279 (1970); W. W. M. Allison, M. Derrick, G. P. Hunt, J. D. Simpson, and L. Voyvodic, *ibid.* 25, 550 (1970).

[6]For a recent review see L. W. Jones, in *Proceedings of the Twelfth International Conference on Cosmic Rays, Hobart, 1971,* edited by A. G. Fenton and K. B. Fenton (Univ. of Tasmania Press, Hobart, Tasmania, 1971).

[7]R. Hagedorn, Nuovo Cimento Suppl. VI, 311 (1968).

[8]Yu. M. Antipov, V. N. Bolotov, N. K. Vishnevskiĭ, M. I. Devishev, M. N. Devisheva, F. A. Ech, A. M. Zaĭtsev, V. V. Isakov, I. I. Karpov, V. A. Krendelev, L. G. Landsberg, V. G. Lapshin, A. A. Lebedev, A. G. Morozov, Yu. D. Prokoshkin, V. G. Rybakov, V. I. Rykalin, A. V. Samoilev, V. A. Sen'ko, and Yu. S. Khodyrev, Yad. Fiz. 10, 976 (1969) [Sov. J. Nucl. Phys. 10, 561 (1970)]; and Yu. M. Antipov *et al.*, Yad. Fiz. 10, 346 (1969) [Sov. J. Nucl. Phys. 10, 199 (1970)].

[9]Yu. M. Bushnin, Yu. P. Gorin, S. P. Denisov, S. V. Donskov, A. F. Dunaĭtsev, V. A. Kachanov, V. I. Kotov, V. M. Kut'in, A. I. Petrukhin, Yu. D. Prokoshkin, E. A. Razuvaev, D. A. Stoyanova, Yu. S. Khodyrev, R. S. Shuvalov, J. V. Allaby, F. Binon, A. M. Wetherell, G. Giacomelli, A. N. Diddens, P. Duteil, R. Meunier, J.-P. Piegneux, M. Spighel, K. A. Stahlbrandt, J.-P. Stroot, and K. Schlupmann, Yad. Fiz. 10, 585 (1969) [Sov. J. Nucl. Phys. 10, 337 (1970)].

[10]S. D. Drell, Phys. Rev. Lett. 5, 278 (1960).

[11]A. Boyarski, F. Bulos, W. Busza, D. Coward, R. Diebold, J. Litt, A. Minten, B. Richter, and R. Taylor, Phys. Rev. Lett. 18, 363 (1967); S. M. Flatté, R. A. Gearhart, T. Hauser, J. J. Murray, R. Morgado, M. Peters, P. R. Klein, L. H. Johnston and S. G. Wojcicki, *ibid.* 18, 366 (1967).

[12]P. Stichel and M. Scholz, Nuovo Cimento 34, 1381 (1964).

[13]D. E. Dorfan, J. Eades, L. M. Lederman, W. Lee, and C. C. Ting, Phys. Rev. Lett. 14, 999 (1965).

[14]M. Danos and B. J. Gibson, Phys. Rev. Lett. 26, 473 (1971).

[15]G. Bathow, E. Freytag, D. H. Schulz, and K. Tesch, Phys. Lett. 25B, 163 (1967); J. Foss, D. Garelick, S. Homma, W. Lobar, L. S. Osborne, and J. Uglum, *ibid.* 25B, 166 (1967); E. H. Bellamy, R. Hofstadter, W. L. Lakin, M. L. Perl, and W. T. Toner, Phys. Rev. 166, 1391 (1968).

[16]T. Massam and A. Zichichi, Nuovo Cimento 43, 2611 (1966).

[17]R. S. Larsen and D. Horelick, in *Proceedings of the Symposium on Beam Intensity Measurement, Dares-*

bury, 1968, edited by V. W. Hatton and S. A. Lowndes (Daresbury Nuclear Physics Laboratory, Daresbury, Lancashire, England, 1968).
[18]G. E. Fischer and Y. Murata, Nucl. Instrum. Methods 78, 25 (1970).
[19]C. K. Sinclair, private communication.
[20]R. A. Early, SLAC Technical Note No. SLAC-TN-66-15 (unpublished).
[21]W. K. H. Panofsky, in *Proceedings of the Conference on Instrumentation for High Energy Physics, Dubna, 1970*, edited by V. Z. Dzhelepov (Joint Institute for Nuclear Research, Dubna, USSR, 1971).
[22]R. M. Sternheimer, Physics 103, 511 (1956).
[23]For relativistic particles the distribution of L. Landau [J. Phys. 8, 201 (1944)], as tabulated by W. Borsch-Supan [J. Res. Natl. Bur. Stand. 65B, 245 (1961)], is used. For other particles the distribution of P. V. Vavilov, Zh. Eksp. Teor. Fiz. 32, 920 (1957) [Sov. Phys.—JETP 5, 749 (1957)], is used.
[24]D. Porat and D. Ouimette, SLAC Technical Note No. SLAC-TN-71-13 (unpublished).
[25]K. J. Kim and Y.-S. Tsai, Phys. Rev. D 8, 3109 (1973).

PHYSICAL REVIEW D VOLUME 9, NUMBER 7 1 APRIL 1974

Pion production in pp collisions at 102 GeV/c*

C. M. Bromberg, D. Chaney, D. Cohen,† T. Ferbel,‡ and P. Slattery
University of Rochester, Rochester, New York 14627

J. W. Chapman, J. W. Cooper, N. Green, A. A. Seidl, and J. C. Vander Velde
University of Michigan, Ann Arbor, Michigan 48104
(Received 2 November 1973)

We present preliminary results on single-pion production and two-pion correlations making use of a 30 000-picture exposure of the ANL/NAL 30-in. hydrogen bubble chamber to 102-GeV/c protons. The data, when compared with those from lower energies, indicate approximate scaling of π^- production in the proton-fragmentation region, but show a continuing rise of the cross section at $y_{\text{c.m.}} = 0$. Stronger correlations are observed between pions of opposite charge than between pions of like charge. The variation with energy of the charge transferred between c.m. hemispheres is slow, as would be predicted by multiperipheral-type models.

I. INTRODUCTION

We present the results of a preliminary investigation of π^+ and π^- production in pp collisions at 102 GeV/c. The data are from the complete measurement of a sample of film containing ~650 events, plus an additional 1200 events belonging to ≤8-pronged topologies, which were obtained in a 30 000-picture exposure of the ANL/NAL 30-in. bubble chamber to 102-GeV/c protons. All tracks from these events were measured in three views using standard 2.5-μ least-count digitizing stages. A special program was written to match the tracks prior to their spatial reconstruction using the TVGP system. The inclusive spectra displayed were obtained by weighting the reconstructed events by the known topological cross sections.[1] The rapidity variable

$$y = \tfrac{1}{2}\ln\left(\frac{E + p_l}{E - p_l}\right)$$

was chosen to display the data. The rapidity of a high-momentum track is rather insensitive to momentum errors.[2] This property, coupled with the excellent pattern recognition capabilities of the 30-in. bubble chamber and its good measurement resolution for low-momentum tracks, allowed us to carry out pion rapidity measurements over the entire kinematic range available at our energy. The systematic errors for the pion rapidity spectra are dominated by corrections due to heavy-particle contamination as discussed in Sec. II.

II. SINGLE-PARTICLE SPECTRA

Corrections for K^- and $\bar{p}$ contamination in the π^- spectra, and for K^+ and high-momentum proton contamination in the π^+ spectra, were applied to the single-particle inclusive data. These corrections were made by generating, through a Monte Carlo program, $K^\pm$ spectra according to the observed K_S^0 data.[3] The energies of the generated $K^\pm$ tracks were subsequently changed by altering the mass hypothesis to be a $\pi^\pm$. These spectra were then subtracted from the measured negative and positive particle distributions. We used a K^+ (K^-) production cross section equal to 1.2 (0.8) times the observed K_S^0 cross section.[4] The $\bar{p}$ contribution was taken to be 20% of the K^- yield. Identifiable protons were removed from the data, and the high-momentum proton subtraction was